

# Geometric Formulation of Unified Force-Impedance Control on $SE(3)$ for Robotic Manipulators

Joohwan Seo<sup>1</sup>, Nikhil Potu Surya Prakash<sup>1</sup>, Soomi Lee<sup>1</sup>, Arvind Kruthiventy<sup>1</sup>, Megan Teng<sup>1</sup>,  
Jongun Choi<sup>1,2</sup> and Roberto Horowitz<sup>1</sup>

**Abstract**—In this paper, we present an impedance control framework on the  $SE(3)$  manifold, which enables force tracking while guaranteeing passivity. Building upon the unified force-impedance control (UFIC) and our previous work on geometric impedance control (GIC), we develop the geometric unified force impedance control (GUFIC) to account for the  $SE(3)$  manifold structure in the controller formulation using a differential geometric perspective. As in the case of the UFIC, the GUFIC utilizes energy tank augmentation for both force-tracking and impedance control to guarantee the manipulator’s passivity relative to external forces. This ensures that the end effector maintains safe contact interaction with uncertain environments and tracks a desired interaction force. Moreover, we resolve a non-causal implementation problem in the UFIC formulation by introducing velocity and force fields. Due to its formulation on  $SE(3)$ , the proposed GUFIC inherits the desirable  $SE(3)$  invariance and equivariance properties of the GIC, which helps increase sample efficiency in machine learning applications where a learning algorithm is incorporated into the control law. The proposed control law is validated in a simulation environment under scenarios requiring tracking an  $SE(3)$  trajectory, incorporating both position and orientation, while exerting a force on a surface. The codes are available at [https://github.com/Joohwan-Seo/GUFIC\\_mujooco](https://github.com/Joohwan-Seo/GUFIC_mujooco).

## I. INTRODUCTION

After its introduction, impedance control [1] has been utilized as a primary control scheme for robotic manipulation tasks that involve interaction with unknown environments. Often combined with an operational space formulation [2], impedance control is also widely utilized to control the manipulator’s end-effector. As impedance/admittance control ensures safe interaction with the environment, it is employed as a low-level control law in recent learning-based policies [3].

Recent advancements in deep-learning approaches showed impressive results in performing real-life tasks. In particular, imitation learning-based policies, such as behavior transformer [4], diffusion policy [5], action-chunking transformer [6], and their variants, have demonstrated success by producing desired end-effector trajectories from vision inputs.

Joohwan Seo, Soomi Lee, Arvind Kruthiventy, and Roberto Horowitz are partially funded by the Hong Kong Center for Construction Robotics Limited. Jongun Choi was supported by the Ministry of Education of the Republic of Korea and the National Research Foundation of Korea. (NRF) (No.RS-2024-00344732)

<sup>1</sup>Department of Mechanical Engineering, University of California, Berkeley {joohwan.seo, nikhilps, soomillee, arvindrkruthiventy, meganteng, horowitz}@berkeley.edu

<sup>2</sup>School of Mechanical Engineering, Yonsei University joungeunchoi@yonsei.ac.kr

Despite the success of those works for real-life tasks, the policies that provide a desired pose may not suffice for high-precision and contact-rich tasks. Because of this limitation, recent works also proposed to output the impedance/admittance gains [7], [8] or direct force profiles [9]. Although changing gains or applying direct force in addition to the designated pose improves the performance for contact-rich tasks, such approaches introduce challenges in guaranteeing stability. Changing impedance/admittance gains during the task execution is generally referred to as variable impedance control [10]. However, from a control-theoretic perspective, the stability result of the original static gain impedance/admittance controller cannot be guaranteed when the gains change [11].

The stability analysis of a robot interacting with the environment is often nested with the concept of passivity. This is due to the fact that the passivity theorem can provide stability guarantees of the overall robot/ environment interaction dynamics, if the robot’s closed-loop system is designed to be passive, since the environment is strictly passive [12], [13], [14]. [15], [16] illustrate the use of closed-loop passivity in the design and implementation of learning controllers for self-optimizing exercise machines, where safe human-machine interaction is indispensable. Other passivity-based control design examples include [17], [18], [19].

In [20], the unified force-impedance control (UFIC) was proposed as a means for a robot manipulator to maintain contact with the environment while executing a task using impedance control and exerting a desired force. Using energy tank augmentation, the UFIC control ensures the passivity of the closed-loop system. However, the UFIC does not consider the  $SE(3)$  manifold structure inherent in the manipulator’s end effector pose description and simply treats pose misalignment errors as Cartesian vectors. Another drawback in [20] is that, in order to establish the passivity of the impedance control term using tank augmentation, a modified desired velocity must be defined, and then it must be integrated to generate a new trajectory. This complicates the update of the next step’s desired velocity and could lead to a causality breakdown in the control process. This is further discussed in Section III-B.3.

Our previous work on geometric impedance control (GIC) [21], [22] established a unified framework for controlling the end-effector’s position and orientation using differential geometry. A significant advantage of the GIC framework is that, as shown in [23], considering the  $SE(3)$  manifold struc-

ture in the control structure leads to  $SE(3)$  invariance and equivariance in the learned policy, which greatly enhances sample efficiency and robustness to out-of-distribution data in deep learning models. The advantages of  $SE(3)$  equivariance in increasing sample efficiency and robustness to out-of-distribution data in visual manipulation learning models have also been recently demonstrated [24], [25], [26], [27].

In this paper, we present a geometric formulation of the unified force-impedance control scheme on the  $SE(3)$  manifold for a robotic manipulator, namely a geometric unified force-impedance control (GUFIC). The key contributions of our paper can be summarized as follows:

- 1) Unlike [20], where translation and the orientation errors are handled separately as if they were elements in vector spaces, we fully incorporate the manifold structure of  $SE(3)$ , and handled translation and orientation errors consistently within the  $SE(3)$  Lie group structure.
- 2) We introduce a time-dependent velocity field to encode a task and derive the trajectory. Consequently, any adjustments to the velocity field preserve causality, which resolves the implementation difficulties in [20].
- 3) Since we follow the formulation of [23], the resulting control law is  $SE(3)$ -equivariant, thus providing further advantages in learning transferability and sample efficiency for learning manipulation tasks.
- 4) From the perspective of the learning manipulation tasks incorporating forces, the passive behavior of the control formulation will further provide advantages such as contact stability.

This paper is organized as follows. In Section II, we provide a brief preliminary background in Lie groups & algebras, manipulator dynamics, and geometric impedance control (GIC). Next, we introduce our GUFIC framework and show its passivity property in Section III. Simulation results follow in Section IV, validating force tracking and motion tracking properties on  $SE(3)$ . Concluding remarks are provided in Section V.

## II. PRELIMINARIES

### A. Lie Groups and Lie Algebra

The configuration of the manipulator's end-effector can be defined by its position and orientation. Among many other representations, such as Euler angles and quaternions for orientations, we are interested in a unified representation of position and orientation, i.e., the Special Euclidean group  $SE(3)$ . We describe the end-effector's configuration through the homogeneous coordinate transformation matrix  $g_{se}$  from the end effector frame  $\{e\}$  to a fixed (inertial) spatial frame  $\{s\}$

$$g_{se} = \begin{bmatrix} R & p \\ 0 & 1 \end{bmatrix} \in SE(3), \quad (1)$$

where  $R$  is a rotation matrix and  $R \in SO(3)$ , and  $p \in \mathbb{R}^3$ . Note that this matrix representation in (1) is known as homogeneous matrix representation. We will drop the subscript  $s$  since the spatial coordinate frame can be considered as an

identity without loss of generality. In addition, we drop the subscript  $e$  for the current configuration of the end-effector for notational compactness unless specified, i.e.,  $g_{se} = g$ . We use  $g = (p, R)$  for notational compactness.

The Lie algebra of  $SE(3)$ ,  $se(3)$ , can be represented by

$$\hat{\xi} = \begin{bmatrix} \hat{\omega} & v \\ 0 & 0 \end{bmatrix} \in se(3), \quad \forall \xi = \begin{bmatrix} v \\ \omega \end{bmatrix} \in \mathbb{R}^6, \quad v, \omega \in \mathbb{R}^3, \quad \hat{\omega} \in so(3).$$

For the details of the Lie group for robotic manipulators, we refer to [28], [29]. Note also that we utilize the standard hat-map and vee-map notations as defined in [21]. We also note that  $se(3)$  is isomorphic to  $\mathbb{R}^6$ .

### B. Manipulator Dynamics

Without loss of generality, we consider the manipulator dynamics of a revolute joint arm

$$M(q)\ddot{q} + C(q, \dot{q})\dot{q} + G(q) = T + T_e, \quad (2)$$

where  $q = [q_1, \dots, q_n]^T \in \mathcal{S}$  with  $\mathcal{S} \triangleq \mathbb{S}^1 \times \dots \times \mathbb{S}^1$  (repeated  $n$  times) are the joint coordinates,  $M(q) \in \mathbb{R}^{n \times n}$  is the symmetric positive definite inertia matrix,  $C(q, \dot{q}) \in \mathbb{R}^{n \times n}$  is the Coriolis matrix,  $G(q) \in \mathbb{R}^n$  is the moment term due to gravity,  $T \in \mathbb{R}^n$  is the control input joint torque, and  $T_e \in \mathbb{R}^n$  is the joint torque due to external disturbances. The  $SE(3)$ -operational space dynamics relative to the end-effector's body-frame is as follows [22]:

$$\begin{aligned} \tilde{M}(q)\dot{V}^b + \tilde{C}(q, \dot{q})V^b + \tilde{G}(q) &= F + F_e, \quad \text{where} \quad (3) \\ \tilde{M}(q) &= J_b(q)^{-T} M(q) J_b(q)^{-1}, \\ \tilde{C}(q, \dot{q}) &= J_b(q)^{-T} (C(q, \dot{q}) - M(q) J_b(q)^{-1} \dot{J}) J_b(q)^{-1}, \\ \tilde{G}(q) &= J_b(q)^{-T} G(q), \quad F = J_b(q)^{-T} T, \quad F_e = J_b(q)^{-T} T_e. \end{aligned}$$

and  $J_b(q)$  is the end-effector body frame Jacobian matrix, i.e.,

$$V^b = \begin{bmatrix} v^b \\ \omega^b \end{bmatrix} = J_b(q)\dot{q}, \quad (4)$$

where the superscript  $b$  denotes that the vector is defined on the body-frame,  $v^b$  and  $\omega^b$  are translational and orientational velocities, respectively.

Note that in our paper [21], we used the symbol  $\tilde{T}$  to represent the wrench in the  $se(3)^*$  end-effector space but we will use the symbol  $F$ , following the notation in [20], to show the direct connection to the UFIC formulation. In addition, we define  $F_e$  to be an external wrench that the environment exerts on the robot, which is opposite to the desired wrench. We also note that we will frequently drop joint coordinate and joint velocities dependences for compactness, unless is necessary for clearness, for example,  $\tilde{M} = \tilde{M}(q)$  and  $\tilde{C} = \tilde{C}(q, \dot{q})$ .

### C. Geometric Impedance Control

In [21], [22], the geometric impedance control (GIC) is proposed to control the position and orientation of the end-effector on the  $SE(3)$  manifold. In summary, the GIC control law is given as follows:

$$F_i = \tilde{M}\dot{V}_d^* + \tilde{C}V_d^* + \tilde{G} - f_g(g, g_d) - K_d e_V, \quad (5)$$

where  $g = (p, R)$  is the current end-effector configuration,  $g_d = (p_d, R_d)$  is the desired configuration,  $g, g_d \in SE(3)$ ,

and  $K_d \in \mathbb{R}^{6 \times 6}$  is symmetric positive definite damping matrix. Furthermore,  $e_V = V^b - V_d^*$ ,  $V_d^* = \text{Ad}_{g_{ed}} V_d^b$ ,  $g_{ed} = g^{-1}g_d$  and  $\text{Ad} : SE(3) \times \mathbb{R}^6 \rightarrow \mathbb{R}^6$  is a large adjoint map, given as

$$\text{Ad}_g = \begin{bmatrix} R & \hat{p}R \\ 0 & R \end{bmatrix}. \quad (6)$$

We use  $V_d^*$ , asterisk notation, to denote that the desired body-frame velocity is translated to the current configuration. We will use the same notation for the generalized vector or co-vector. The  $f_g$  term in (5) is the elastic force in  $SE(3)$ :

$$f_g(g, g_d) = \begin{bmatrix} f_p(g, g_d) \\ f_R(g, g_d) \end{bmatrix} = \begin{bmatrix} R^T R_d K_p R_d^T (p - p_d) \\ (K_R R_d^T R - R^T R_d K_R)^\vee \end{bmatrix}, \quad (7)$$

where  $K_p, K_R \in \mathbb{R}^{3 \times 3}$  are symmetric positive stiffness matrices for the translational and rotational dynamics, respectively.

The GIC control law (5) is formulated using potential energy and kinetic energy functions on  $SE(3)$ . We will choose the potential function derived from the Lie group, among other possible choices for potential energy functions [22]. Thus, the error potential function  $P(t, q)$  and the error kinetic energy function  $K(t, q, \dot{q})$  are defined as follows:

$$P(t, q) = \text{tr}(K_R(I - R_d^T R)) + \frac{1}{2}(p - p_d)^T R_d K_p R_d^T (p - p_d) \\ K(t, q, \dot{q}) = \frac{1}{2} e_V^T \tilde{M} e_V, \quad (8)$$

It should be noted that the GIC law is formulated based on the following assumption:

**Assumption 1 ([21]):** The end-effector lies in a region  $D \subset SE(3)$  such that the Jacobian  $J_b$  is full-rank. Moreover, the end-effector of the manipulator and the desired trajectory lies in the reachable set  $\mathcal{R}$ , i.e.,

$$p(q) \in \mathcal{R} = \{p(q) \mid \forall q \in \mathcal{S}\} \subset \mathbb{R}^3,$$

and the desired trajectory is also continuously differentiable.

Based on the GIC law, we have developed a learning variable impedance control to solve the peg-in-hole task problem [23], showing that the resulting method is  $SE(3)$  equivariant. However, when the impedance gain changes, the stability property of the original control law may not be valid, as noted in [11]. In fact, the stable behavior of the control system in interaction with the external environment can be better understood by the energetic passivity property [30], [12]. On the other hand, from the perspective of the assembly task, the objective of variable impedance control in the end is to adapt to the external force [31], which implies that formulating variable impedance control into a control that allows direct force feedback may be more favorable.

Therefore, the following section introduces a Geometric Unified Force-Impedance Control, a force-control augmented GIC that preserves the passivity property using energy-tanks.

### III. GEOMETRIC UNIFIED FORCE IMPEDANCE CONTROL

In this section, we will re-formulate the original unified force-impedance control (UFIC) [20], so that the manifold structure of  $SE(3)$  of the end-effector can be fully taken into account. By formulating into the GIC form, the resulting

control framework enjoys the  $SE(3)$ -equivariance property as suggested in [23], when it is augmented with learning.

#### A. Naive Force Tracking Control Law

In this section, we will augment the geometric impedance control  $F_i$  in (5) with the force tracking control  $F_f$  so that the total input control wrench is

$$F = F_i + F_f, \quad (9)$$

where  $T_f = J_b^T F_f$ , and

$$F_f = -k_p(-\bar{F}_e - F_d) - k_d \frac{d}{dt}(-\bar{F}_e - F_d) \\ - k_i \int (-\bar{F}_e(\tau) - F_d(\tau)) d\tau + F_d. \quad (10)$$

As in [20], we use  $\bar{F}_e = \bar{F}_e(t)$  for the force/torque sensor output, without discerning it from  $F_e$  the actual external wrench that the environment exerts on the robot  $F_e$ . We also define  $F_d = F_d(t, g)$  to denote the desired force field. The details about the force field formulation will be further addressed in a later Section. However, as will be shown in the following, the naive force-impedance control law (9) is not passive.

1) *Passivity Analysis:* The control system is passive with respect to the pair  $(V^b, F_e)$ , or the supply rate  $(V^b)^T F_e$ , when the following condition is satisfied:

$$\dot{S} \leq (V^b)^T F_e, \quad (11)$$

where  $S \in \mathbb{R}_{\geq 0}$  is a positive definite storage function. Noting that the force exerted on the environment is  $-F_e$ , the passivity condition for the environment is given as

$$\dot{S}_{env} \leq (V^b)^T (-F_e), \quad (12)$$

i.e., it should be passive under the pair  $(V^b, -F_e)$ . The error dynamics with the naive geometric force-impedance control law can be written by

$$\tilde{M}\dot{e}_V + \tilde{C}e_V + K_d e_V + f_g - F_f - F_e = 0. \quad (13)$$

Following the formulation from [21], we will use the summation of the potential energy function in  $SE(3)$  and kinetic energy function as the storage function, i.e.,

$$S(t, q, \dot{q}) = K(t, q, \dot{q}) + P(t, q), \quad (14)$$

where  $K$  and  $P$  are defined in (8). Using the fact that  $\dot{P} = f_g^T e_V$  from [21], [22], one can further show that

$$\frac{dS}{dt} = e_V^T \tilde{M}\dot{e}_V + \frac{1}{2} e_V^T \dot{\tilde{M}} e_V + f_g^T e_V \\ = e_V^T (-\tilde{C}e_V - K_d e_V - f_g + F_f + F_e + f_g) + \frac{1}{2} e_V^T \dot{\tilde{M}} e_V \\ = \underbrace{e_V^T (\frac{1}{2} \dot{\tilde{M}} - \tilde{C}) e_V}_{=0} - \underbrace{e_V^T K_d e_V}_{\geq 0} + e_V^T F_f + e_V^T F_e \\ \leq (V^b)^T F_e + (V^b)^T F_f - (V_d^*)^T (F_f + F_e). \quad (15)$$

Since the signs of the terms  $(V^b)^T F_f$  and  $(V_d^*)^T (F_f + F_e)$  are not determined, the passivity of the control system cannot be guaranteed.

#### B. Passive Control Law Formulation

In order to make the control system closed loop passive, we will incorporate energy storage, through tank augmen-

tation, for both the force-tracking and the impedance controllers, as in [20].

### 1) Tank Augmentation for Force-tracking Controller:

First, for the port  $(V^b, F_f)$ , the energy tank with respect to the force control  $T_f$  is first defined as

$$T_f = \frac{1}{2} x_{tf}^2, \quad x_{tf} \neq 0, \quad (16)$$

with the tank state dynamics

$$\dot{x}_{tf} = -\frac{\beta_f}{x_{tf}} \gamma_f (V^b)^T F_f + \frac{\alpha_f}{x_{tf}} (\gamma_f - 1) (V^b)^T F_f, \quad (17)$$

where

$$\gamma_f = \begin{cases} 1 & \text{if } (V^b)^T F_f < 0 \\ 0 & \text{otherwise} \end{cases}, \quad \beta_f = \begin{cases} 1 & \text{if } T_f \leq T_{u,f} \\ 0 & \text{otherwise} \end{cases}$$

$$\alpha_f = \begin{cases} 1 & \text{if } T_f \geq T_{l,f} + \delta_{T,f} \\ \frac{1}{2} \left( 1 - \cos \left( \frac{T_f - T_{l,f}}{\delta_{T,f}} \pi \right) \right) & \text{if } T_{l,f} + \delta_{T,f} \geq T_f \geq T_{l,f} \\ 0 & \text{otherwise,} \end{cases}$$

where  $T_{u,f}$  and  $T_{l,f}$  denote the upper limit and lower limit of the energy tank for force tracking control, respectively, and  $\delta_{T,f}$  is a margin towards the lower limit of the energy tank to enable smooth switching behavior. The purpose of  $\gamma_f$  is an indicator of whether the force tracking law  $F_f$  is in the passivity-violating direction, and  $\beta_f$  is to prevent the overflow of the energy tank. Depending on the energy tank level and  $\gamma_f$  value, the force tracking law  $F_f$  is modified as

$$F'_f = (\gamma_f + \alpha_f(1 - \gamma_f)) F_f. \quad (18)$$

As will be clarified later, the effect of (18) is to guarantee the passivity for the force tracking port  $(V^b, F'_f)$ .

2) *Tank Augmentation for Impedance Controller:* Secondly, to the port  $(V_d^*, -(F'_f + F_e))$ , the energy tank level with respect to the impedance control  $T_i$  is defined as

$$T_i = \frac{1}{2} x_{ti}^2, \quad x_{ti} \neq 0, \quad (19)$$

with the tank state dynamics given by

$$\dot{x}_{ti} = \frac{\beta_i}{x_{ti}} (\gamma_i (V_d^*)^T (F'_f + F_e) + (e'_V)^T K_d e'_V) + \frac{\alpha_i}{x_{ti}} (1 - \gamma_i) (V_d^*)^T (F'_f + F_e), \quad (20)$$

where

$$e'_V = V^b - (\gamma_i + \alpha_i(1 - \gamma_i)) V_d^* = V^b - (V_d^*)'$$

and

$$(V_d^*)' = (\gamma_i + \alpha_i(1 - \gamma_i)) V_d^* \quad (21)$$

is the modified desired velocity.  $\gamma_i$ ,  $\beta_i$  and  $\alpha_i$  are defined respectively as

$$\gamma_i = \begin{cases} 1 & \text{if } (V_d^*)^T (F'_f + F_e) > 0 \\ 0 & \text{otherwise} \end{cases}, \quad \beta_i = \begin{cases} 1 & \text{if } T_i \leq T_{u,i} \\ 0 & \text{otherwise} \end{cases}$$

$$\alpha_i = \begin{cases} 1 & \text{if } T_i \geq T_{l,i} + \delta_{T,i} \\ \frac{1}{2} \left( 1 - \cos \left( \frac{T_i - T_{l,i}}{\delta_{T,i}} \pi \right) \right) & \text{if } T_{l,i} + \delta_{T,i} \geq T_i \geq T_{l,i} \\ 0 & \text{otherwise,} \end{cases}$$

where  $T_{u,i}$  and  $T_{l,i}$  denote the upper limit and lower limit of the energy tank for the impedance control, respectively, and  $\delta_{T,i}$  is a smoothing margin for the impedance control energy tank, analogous to the one for the force tracking control.

3) *Velocity Field and Force Field Formulation:* One subtle challenge arises when implementing the modified desired

velocity  $(V_d^*)'$ : updating the corresponding signals  $(\dot{V}_d^*)'$  and  $g'_d$  accordingly. While the original work [20] suggested integrating and differentiating the modified velocity signal appropriately, naive implementations can easily lead to causality problems, requiring careful engineering to ensure precise updates. Specifically, integrating the modified velocity at the current time step yields an updated trajectory, yet the next-step desired velocity cannot be directly computed in a causal manner. To resolve this issue, we propose employing the notion of a velocity field [12]. Formally, the velocity field  $V_d^*(t, g)$  is defined as a mapping from the current time  $t$  and the current pose  $g \in SE(3)$  to vectors on the Lie algebra  $se(3)$ , ensuring  $g(t) \hat{V}_d^*(t, g) \in T_g SE(3)$ . Thus, our proposed velocity field is expressed as  $\hat{V}_d^* : \mathbb{R}_{\geq 0} \times SE(3) \rightarrow se(3)$ , explicitly dependent on both time and pose rather than solely time.

a) *Velocity Field:* Let us first denote the original time-trajectory as  $\bar{g}_d(t) = (\bar{p}_d(t), \bar{R}_d(t))$  and their corresponding desired body-frame velocity as  $\bar{V}_d^b(t)$ . We will also drop the time dependency to avoid clutter, e.g.,  $\bar{g}_d = \bar{g}_d(t)$ . Following the formulation of [12], together with the touch of manifold sense of  $SE(3)$ , the time-varying velocity field  $\hat{V}_d^*(t, g)$  from the desired trajectory  $\bar{g}_d$  and  $\hat{V}_d^b = \bar{g}_d^{-1} \dot{\bar{g}}_d$  is given by

$$\hat{V}_d^*(t, g) = \bar{g}_{ed} \hat{V}_d^b(t) \bar{g}_{ed}^{-1} + \zeta \nabla_1 \Psi(g, \bar{g}_d), \quad (22)$$

where  $\bar{g}_{ed} = g^{-1} \bar{g}_d$ .  $\Psi(g, \bar{g}_d)$  is an error function given by

$$\Psi(g, \bar{g}_d) = \frac{1}{2} \|I_4 - g_d^{-1} g\|_F^2 = \text{tr}(I - R_d^T R) + \frac{1}{2} \|p - p_d\|_2^2, \quad (23)$$

that can serve as a distance metric on  $SE(3)$ , proposed in [21].  $\zeta \in \mathbb{R}_{>0}$  is a positive scalar gain, and  $\nabla_1$  denotes the gradient to the first argument of the function. One can also notice that from [28] (see Chapter 2.4),

$$\hat{V}_d^* = \bar{g}_{ed} \hat{V}_d^b \bar{g}_{ed}^{-1} \iff \bar{V}_d^* = \text{Ad}_{\bar{g}_{ed}} \bar{V}_d^b.$$

Additionally, it is shown in [21] that

$$\nabla_1 \Psi(g, \bar{g}_d) = \hat{e}_G(g, \bar{g}_d), \quad (24)$$

where  $e_G(g, \bar{g}_d)$  is a geometrically consistent error vector (GCEV) proposed in [23], [21] given by

$$e_G(g, \bar{g}_d) = \begin{bmatrix} R^T(p - p_d) \\ (R_d^T R - R^T R_d)^\vee \end{bmatrix}, \quad (25)$$

see also [32], [33], [34] for more results on  $SE(3)$ , and [35] for the result on  $SO(3)$ .

Now that we are equipped with the velocity field  $V_d^*(t, g)$ , the velocity modification law (21) can be freely applied. Using the modified velocity field for the trajectory tracking  $(\hat{V}_d^*(t, g))'$ , the modified desired configuration  $g'_d(t)$  can be obtained by integrating from

$$\dot{g}'_d = g'_d (\hat{V}_d^b)' , \quad (26)$$

where  $(V_d^b)' = \text{Ad}_{g_{ed}^{-1}} (V_d^*)'$ , which can be discretized via

$$g'_d(t + \Delta t) \cong g_d(t)' \exp \left( \hat{V}_d^b \Delta t \right)'.$$

We emphasize that since the desired pose is now derived from the velocity field, modifying the velocity field and obtaining the desired pose can be performed without losing causality.

The time derivative of the velocity field  $V_d^*$  needs to be directly calculated. The full calculations for  $V_d$  and  $\dot{V}_d^*$  are shown in the Appendix. A.

*b) Force Field:* As the desired velocity is formulated with the field, the desired force can be formulated similarly with the field structure. To allow its maximum freedom, we will formulate the desired force as a time-varying velocity field, i.e.,  $F_d = F_d(t, g) \in T_g^*SE(3)$ , where  $T_g^*SE(3)$  denotes the dual space of  $T_gSE(3)$ . Based on this formulation, one can use a time-dependent desired force by dropping the dependency on the current configuration  $g$ , and vice versa. The other consideration is whether to define the desired force on the point  $g$  or  $g_d$  on the manifold on  $SE(3)$ . When the desired force is represented on the dual space of the desired pose  $g_d$ ,  $F_d(t) \in T_{g_d}^*SE(3)$ , the appropriate coordinate transformation (dual adjoint map)  $\text{Ad}_{g_{ed}}^{*-1}$  [23] needs to be applied, so that:

$$F_d^*(t) = \text{Ad}_{g_{ed}}^* F_d(t) = \text{Ad}_{g_{ed}}^{T^*} F_d(t) \in T_g^*SE(3).$$

In this paper, we will only consider the simple case, where  $F_d$  is constant over space and time.

*4) Final Geometric Unified Force-Impedance Controller:* Using the modified setpoint calculated from the velocity field, the modified impedance controller is formulated as follows:

$$F_i' = \tilde{M}(\dot{V}_d^*)' + \tilde{C}(V_d^*)' + \tilde{G} - f_G(g, g_d') - K_d e_V'. \quad (27)$$

The updated storage function now reads:

$$S = \frac{1}{2}(e_V')^T \tilde{M} e_V' + P(g, g_d'). \quad (28)$$

Combining all together, the final GUFIC is presented:

$$T = J_b^T F', \quad \text{where } F' = F_f' + F_i', \quad (29)$$

where  $F_f'$  and  $F_i'$  are shown in (18) and (27), respectively. The main theorem of the paper is presented:

**Theorem 1 (Passivity of the GUFIC):** Suppose that assumption 1 holds true. Consider a robotic manipulator with dynamics (2) and the GUFIC control law (29). Then, the closed-loop system is passive for the channel  $(V^b, F_e)$ , with respect to the storage function (32).

*Proof:* Using the control law (29), the modified error dynamics reads

$$\begin{aligned} \tilde{M}\dot{V}^b + \tilde{C}V^b + \tilde{G} &= F_f' + F_i' + F_e \\ \implies \tilde{M}\dot{e}_V' + \tilde{C}e_V' + K_d e_V' + f_G(g, g_d') &= F_f' + F_e. \end{aligned} \quad (30)$$

Together with (27), (18), and (26), the time derivative of the storage function is

$$\begin{aligned} \dot{S} &= (e_V')^T \tilde{M}\dot{e}_V' + (e_V')^T \frac{1}{2}\dot{\tilde{M}}e_V' + (e_V')^T f_G(g, g_d') \\ &= (e_V')^T (-\tilde{C}e_V' - f_G(g, g_d') - K_d e_V' + F_f' + F_e) \\ &\quad + \frac{1}{2}\dot{\tilde{M}}e_V' + (e_V')^T f_G(g, g_d') \\ &= -(e_V')^T K_d e_V' + (e_V')^T F_f' + (e_V')^T F_e. \end{aligned} \quad (31)$$

By augmenting the energy tanks  $T_i$  and  $T_f$ , the total storage function  $S_{tot}$  is now

$$S_{tot} = S + T_i + T_f. \quad (32)$$

The time-derivative of the  $T_f = \frac{1}{2}x_{tf}^2$  and  $T_i = \frac{1}{2}x_{ti}^2$  is

derived using (17) and (20) as follows:

$$\begin{aligned} \frac{d}{dt}(T_f + T_i) &= x_{tf}\dot{x}_{tf} + x_{ti}\dot{x}_{ti} \\ &= -\beta_f \gamma_f (V^b)^T F_f + \alpha_f (\gamma_f - 1)(V^b)^T F_f \\ &\quad + \beta_i (\gamma_i (V_d^*)^T (F_f' + F_e) + (e_V')^T K_d e_V') \\ &\quad + \alpha_i (1 - \gamma_i)(V_d^*)^T (F_f' + F_e). \end{aligned} \quad (33)$$

The time derivative of the total storage function is then

$$\begin{aligned} \dot{S}_{tot} &= \dot{S} + \dot{T}_f + \dot{T}_i \\ &= -(e_V')^T K_d e_V' + (V^b)^T F_e + (V^b)^T F_f' - (V_d^*)^T (F_f' + F_e) \\ &\quad - \beta_f \gamma_f (V^b)^T F_f + \alpha_f (\gamma_f - 1)(V^b)^T F_f \\ &\quad + \beta_i (\gamma_i (V_d^*)^T (F_f' + F_e) + (e_V')^T K_d e_V') \\ &\quad + \alpha_i (1 - \gamma_i)(V_d^*)^T (F_f' + F_e). \end{aligned} \quad (34)$$

With some algebra, it follows that

$$\begin{aligned} \dot{S}_{tot} &= \underbrace{\gamma_f (1 - \beta_f)(V^b)^T F_f}_{\leq 0} + \underbrace{(\beta_i - 1)(e_V')^T K_d e_V'}_{\leq 0} \\ &\quad + \underbrace{\gamma_i (\beta_i - 1)(V_d^*)^T (F_f' + F_e)}_{\leq 0} + (V^b)^T F_e. \end{aligned} \quad (35)$$

To elaborate, we can look into the cases when the passivity is violated. For the port  $(V^b, F_f)$ , the value of  $\gamma_f$  depends on the passivity condition. When the passivity condition is satisfied, i.e.,  $(V^b)^T F_f < 0$  then  $\gamma_f = 1$ , and when the passivity is violated then  $\gamma_f = 0$ . The term related to this port in (35) is  $\gamma_f (1 - \beta_f)(V^b)^T F_f$ . As  $(1 - \beta_f) \geq 0$  is always satisfied (since  $\beta_f \in \{0, 1\}$ ), and  $\gamma_f = 0$  if the passivity is violated, we show that:

$$\gamma_f (1 - \beta_f)(V^b)^T F_f \leq 0 \quad (36)$$

holds in every case.

Similarly for the port  $(V_d^*, -(F_f' + F_e))$ ,  $\gamma_i = 1$  only when the passivity condition is satisfied and otherwise 0. As  $(\beta_i - 1) \leq 0$ , one can verify that the terms  $(\beta_i - 1)(e_V')^T K_d e_V' \leq 0$  and  $\gamma_i (\beta_i - 1)(V_d^*)^T (F_f' + F_e) \leq 0$ . Combining these results, it is shown that

$$\dot{S}_{tot} \leq (V^b)^T F_e, \quad (37)$$

which proves that the closed-loop system is passive. ■

**Remark 1 (Stability Result):** Using the result (37), the stability of the system can be proved, similar to [20]. The proof through Lyapunov's direct method can be conducted using the augmented Lyapunov function with the coupling term as in [21], [32]. The main implications of the stability analysis are: 1. The system asymptotically converges to  $g_d'$ , the modified setpoint; 2. When  $g$  converges to  $g_d'$ , the force will also converge to  $F_d = -F_e$ .

**Remark 2 ( $SE(3)$  Invariance and Equivariance):** The proposed GUFIC framework is also  $SE(3)$  invariant. For the terms related to the GIC, the left-invariance follows from the results of Lemma 1 in [23]. The force tracking law and modification of the velocity field and force tracking law are all defined on the body-frame attached to the end-effector, leading to  $SE(3)$  invariance property of the controller. Moreover, since the GUFIC law satisfies  $SE(3)$  left-invariance and is defined on the end-effector body

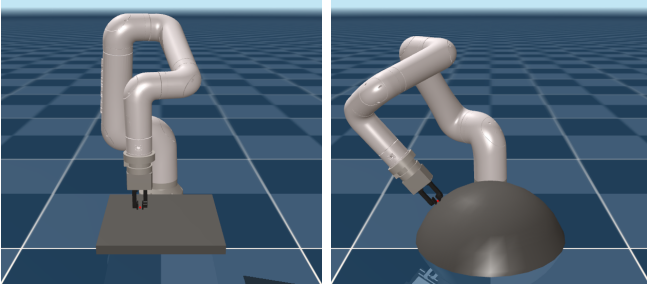


Fig. 1: Implemented Mujoco Simulation Environment with Indy7 robot. (Left) The robot follows a circular trajectory while exerting normal force. (Right) The robot follows a line trajectory on the sphere while exerting normal force.

frame, the control law is  $SE(3)$  equivariant (see Proposition 2 of [23]).

**Remark 3 (Contact-loss Stabilization):** A critical issue in the original tank-augmented UFIC framework arises when force and motion controls become parallel or collinear, notably during the loss of end-effector contact, leading to undesired motions. Although the original paper [20] mentioned that this scenario could be handled by depleting the energy tank to avoid hazardous contact, such an approach may be impractical. Following their recommendation, we adopt a controller shaping function,  $\rho$ , which modulates the force-tracking control law to preserve passivity and manage potential contact-loss situations. While we implement this controller shaping function, detailed analysis of its performance is not our primary contribution. In addition, due to the page limit, we omitted its details and refer readers to [20] for an in-depth discussion of its effectiveness.

#### IV. SIMULATION RESULTS

We implemented the GUFIC control law in the Mujoco environment [36] because it is well-known for handling contact-related simulations. The Indy7 Robot [37] from Neuromeka was incorporated into the Mujoco environment. In this simulation study, we show two force control scenarios: 1. The robot follows a circular trajectory while applying force to the surface; 2. The robot follows a trajectory on a sphere that incorporates  $SE(3)$  motions.

The force-torque sensor value has been passed to 2<sup>nd</sup> order low-pass filter with 5Hz of the cut-off frequency. The sampling frequency of the whole simulation and the control loop was 1000Hz.

##### A. Scenario 1: Circular Trajectory

In this scenario, the robot follows the circular trajectory while applying the force field. As for the benchmark controller, we will use a standard GIC controller. For a standard impedance controller to apply a desired force against a surface, precise information on the surface's geometry or adaptation law is required. In this scenario, we assume that the GIC controller does not have accurate information but only a rough guess, leading to incorrect force exertion. In particular, the desired trajectory  $\bar{g}_d(t) = (\bar{p}_d(t), \bar{R}_d(t))$  is

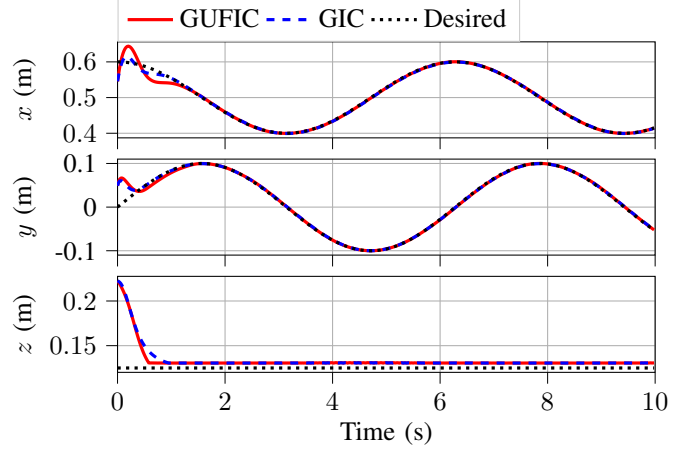


Fig. 2: Trajectory tracking results of GUFIC and GIC for Scenario 1.

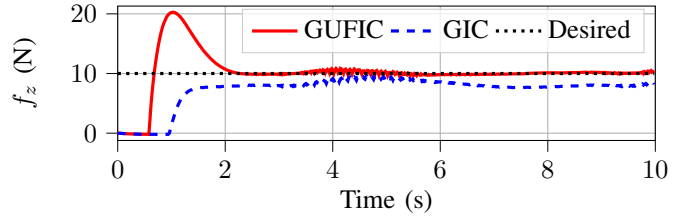


Fig. 3: Force tracking result of GUFIC and GIC for Scenario 1.

given as

$$\bar{p}_d(t) = \begin{bmatrix} 0.5 + 0.1 \cos t \\ 0.1 \sin t \\ 0.125 \end{bmatrix}, \quad \bar{R}_d(t) = \begin{bmatrix} 0 & 1 & 0 \\ 1 & 0 & 0 \\ 0 & 0 & -1 \end{bmatrix} \quad (38)$$

Notice that the center position of the surface is given as  $p_{surface} = [0.5, 0.0, 0.1308]^T$  and that the goal position for both GIC and GUFIC is inside the surface to make a proper contact. The gains for the GUFIC are given by  $K_p = \text{blkdiag}([2000, 2000, 10])$ ,  $K_R = \text{blkdiag}([2000, 2000, 2000])$ ,  $(k_p, k_i, k_d) = (1.0, 0.5, 4.0)$ , and  $K_d = 500I_{6 \times 6}$ . For the velocity field generation,  $\zeta = 5$  was used. For the GIC, the same gain values are used with GUFIC except  $K_p = \text{blkdiag}([2500, 2500, 1500])$ , and without using PID gains for force-tracking control. The initial values of the tanks are selected for 10, with the lower value of  $T_{l,i} = T_{l,f} = 0.1$ , the upper value  $T^{u,i} = T^{u,f} = 20$ , and the buffer  $\delta_{T,i} = \delta_{T,f} = 0.5$ . The force field is selected as  $F_d(t, g) = [0, 0, 10, 0, 0, 0]^T$ .

The trajectory tracking results from the first scenario are

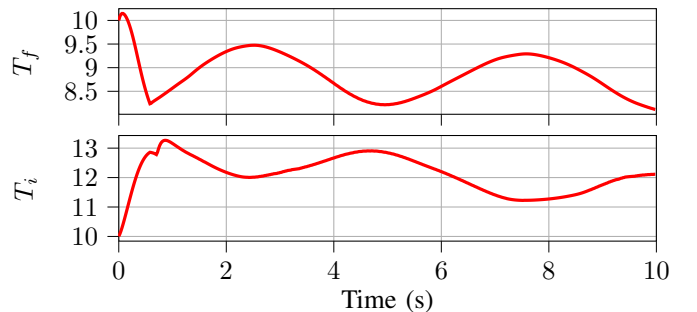


Fig. 4: Energy Tanks  $T_f$  and  $T_i$  of GUFIC for Scenario 1.

shown in Fig. 2. As can be noticed, both approaches showed almost perfect trajectory tracking results. The force tracking result in the surface normal direction is shown in Fig. 3. As the GIC only has rough information on the surface, the gain values required for the desired force are unknown, leading to a significant steady-state error in tracking the desired force. The tank values during the task are shown in Fig. 4. As the tank values are not depleted during the execution of the task it can be successfully accomplished.

### B. Scenario 2: Line Trajectory on the Sphere

In this scenario, the controller tries to follow the trajectory on a sphere while exerting a normal force. Specifically, the desired trajectory  $\bar{g}_d(t)$  is fed as follows:

$$\bar{p}_d(t) = [0.4, 0 + 0.3 \sin \theta(t), -0.1 + 0.3 \cos \theta(t)]^T, \quad (39)$$

$$\bar{R}_d(t) = \begin{bmatrix} 0 & 1 & 0 \\ 1 & 0 & 0 \\ 0 & 0 & -1 \end{bmatrix} \cdot \begin{bmatrix} \cos(-\theta(t)) & 0 & \sin(-\theta(t)) \\ 0 & 1 & 0 \\ -\sin(-\theta(t)) & 0 & \cos(-\theta(t)) \end{bmatrix},$$

where  $\theta(t) = -\frac{\pi}{4} + \frac{\pi}{20}t$ . Notice that we have used the same gain values as in the Scenario 1, except for the PID gains for the force tracking controller. The gains used in this scenario are  $(k_p, k_i, k_d) = (1.5, 0.75, 6.0)$ . The impedance tank's initial value was 90, with the upper bound  $T^{u,i}$  being 100.

The trajectory tracking results for the second scenario are presented in Fig. 5 and showed perfect trajectory tracking results for the  $x$  and  $y$  direction, but in the  $z$  direction there is a slight steady-state error because of imperfect information regarding the sphere. The error function  $\Psi$  (23) is shown in Fig. 6, showing the convergence of the tracking errors on both the translational and rotational dynamics. The force tracking results are plotted in Fig. 7, showing convergence for the GUFIC but significant error for the GIC. The energy tanks  $T_f$  and  $T_i$  are presented in Fig. 8. The impedance control tank  $T_i$  reduces rapidly as the feedforward velocity  $V_d^*$  is in the passive-violation direction. We therefore set a significantly higher initial value  $T_i(0)$  to prevent depletion than in the previous scenario. As already pointed out in [20], when the impedance tank  $T_i$  is depleted, the modified desired velocity field  $(V_d^*)'$  becomes zero, leading to the static desired pose, i.e.,  $g_d(k+1) = g_d(k)$ . Similarly, when the force control tank  $T_f$  is depleted, the modified force control  $(F_f)'$  becomes zero.

## V. CONCLUSION AND FUTURE WORKS

This paper proposes a geometric unified force-impedance control (GUFIC) framework that fully exploits the  $SE(3)$  manifold structure to achieve robust force tracking while ensuring passivity. The proposed approach ensures safe interaction with uncertain environments by augmenting energy tanks to the controller. Furthermore, the introduction of velocity and force fields resolves the non-causal implementation issues present in earlier frameworks. The control design inherits  $SE(3)$  invariance and equivariance properties by formulating the unified force-impedance control through differential geometric methods, improving learning sample

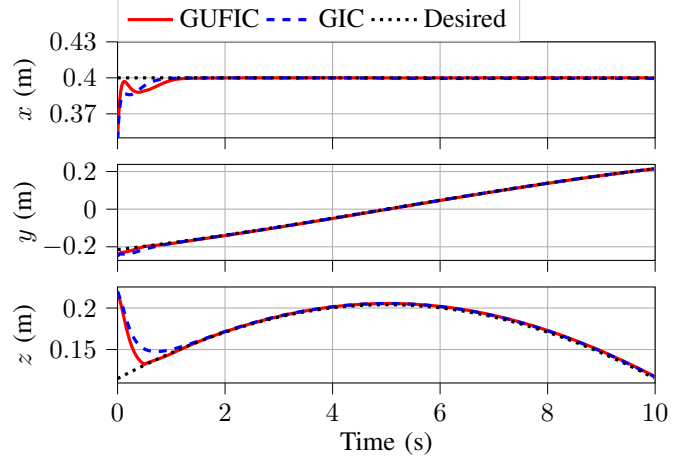


Fig. 5: Trajectory tracking results of GUFIC for Scenario 2.

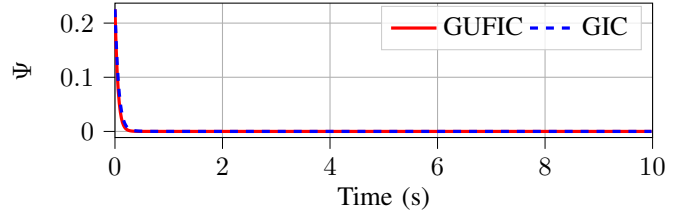


Fig. 6: Error Function  $\Psi$  (23) of GUFIC for Scenario 2.

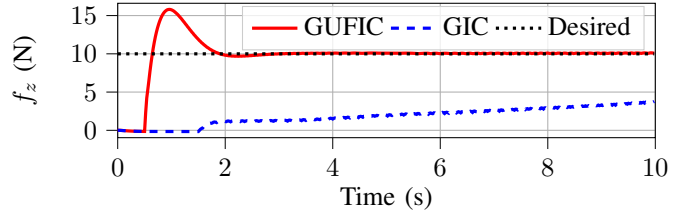


Fig. 7: Force tracking result of GUFIC for Scenario 2.

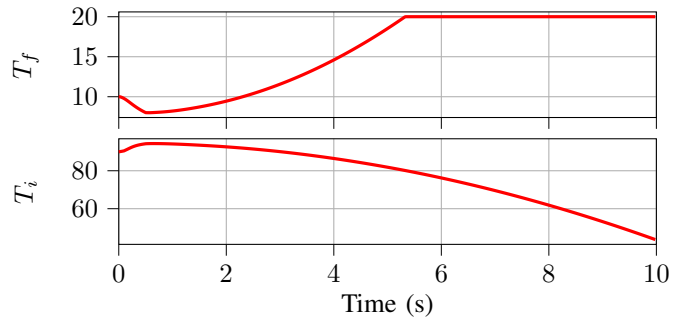


Fig. 8: Energy Tanks  $T_f, T_i$  of GUFIC for Scenario 2.

efficiency. Simulation results have validated the effectiveness of GUFIC in executing complex  $SE(3)$  motions, demonstrating its capability to track trajectories with both position and orientation changes while maintaining the desired force profile.

Although we assumed in this paper that the velocity and force fields are defined in advance and provided, an interesting question arises on whether these fields could be learned from experts' demonstrations. In this regard, our future work will focus on learning velocity and force fields via imitation learning using equivariant learning methods, so



that the whole model pipeline can guarantee passivity and equivariance.

## APPENDIX

### A. Time-derivative of the velocity field $V_d^*$

The proposed velocity field (22) reads

$$\begin{aligned}\hat{V}_d^*(t, g) &= \bar{g}_{ed} \hat{V}_d^b(t) \bar{g}_{ed}^{-1} + \zeta \hat{e}_G(g, \bar{g}_d) \\ &= \begin{bmatrix} R^T \dot{R}_d \bar{R}_d^T R & R^T \dot{R}_d \bar{R}_d^T (p - \bar{p}_d) + R^T \dot{p}_d \\ 0 & 0 \end{bmatrix} \\ &\quad - \zeta \begin{bmatrix} \bar{R}_d^T R - R^T \bar{R}_d & R^T (p - \bar{p}_d) \\ 0 & 0 \end{bmatrix}.\end{aligned}$$

The time derivatives of each term can be straightforwardly obtained as follows:

$$\begin{aligned}\frac{d}{dt}(R^T \dot{R}_d \bar{R}_d^T R) &= -\dot{\omega}^b R^T \dot{R}_d \bar{R}_d^T R + R^T \ddot{R}_d \bar{R}_d^T R + R^T \dot{R}_d \dot{\bar{R}}_d^T R + R^T \dot{R}_d \bar{R}_d^T R \dot{\omega}^b \\ \frac{d}{dt}(R^T \dot{R}_d \bar{R}_d^T (p - \bar{p}_d) + R^T \dot{p}_d) &= -\dot{\omega}^b R^T \dot{R}_d \bar{R}_d^T (p - \bar{p}_d) + R^T \ddot{R}_d \bar{R}_d^T (p - \bar{p}_d) + R^T \dot{R}_d \dot{\bar{R}}_d^T (p - \bar{p}_d) \\ &\quad + R^T \dot{R}_d \bar{R}_d^T (R^T v - \dot{p}_d) - \dot{\omega}^b R^T \dot{p}_d + R^T \ddot{p}_d \\ \frac{d}{dt}(\bar{R}_d^T R - R^T \bar{R}_d) &= \dot{\bar{R}}_d^T R + R_d^T R \dot{\omega}^b + \dot{\omega}^b R^T R_d - R^T \dot{R}_d \\ \frac{d}{dt}(R^T (p - \bar{p}_d)) &= -\dot{\omega}^b R^T (p - \bar{p}_d) + v - R^T \dot{p}_d\end{aligned}$$

Note that  $V^b = [(v^b)^T, (\omega^b)^T]^T$  is obtained from  $V^b = J_b(q)\dot{q}$  and that  $\dot{R} = R\dot{\omega}^b$  and  $\dot{p} = R^T v$  are utilized. Also note that time derivatives of  $R_d$  and  $p_d$  can be obtained from the trajectory signals.

## REFERENCES

- [1] N. Hogan, "Impedance control: An approach to manipulation: Part ii—implementation," 1985.
- [2] O. Khatib, "A unified approach for motion and force control of robot manipulators: The operational space formulation," *IEEE Journal on Robotics and Automation*, vol. 3, no. 1, pp. 43–53, 1987.
- [3] M. Bogdanovic *et al.*, "Learning variable impedance control for contact sensitive tasks," *IEEE Robotics and Automation Letters*, vol. 5, no. 4, pp. 6129–6136, 2020.
- [4] N. M. Shafiullah *et al.*, "Behavior transformers: Cloning  $k$  modes with one stone," *Advances in neural information processing systems*, vol. 35, pp. 22955–22968, 2022.
- [5] C. Chi *et al.*, "Diffusion policy: Visuomotor policy learning via action diffusion," *The International Journal of Robotics Research*, p. 02783649241273668, 2023.
- [6] Z. Fu *et al.*, "Mobile aloha: Learning bimanual mobile manipulation with low-cost whole-body teleoperation," *arXiv preprint arXiv:2401.02117*, 2024.
- [7] B. Zhou *et al.*, "Admittance visuomotor policy learning for general-purpose contact-rich manipulations," *arXiv preprint arXiv:2409.14440*, 2024.
- [8] T. Kamijo *et al.*, "Learning variable compliance control from a few demonstrations for bimanual robot with haptic feedback teleoperation system," in *2024 IEEE/RSJ International Conference on Intelligent Robots and Systems (IROS)*. IEEE, 2024, pp. 12663–12670.
- [9] Y. Wu *et al.*, "Tacdiffusion: Force-domain diffusion policy for precise tactile manipulation," *arXiv preprint arXiv:2409.11047*, 2024.
- [10] M. Suomalainen *et al.*, "A survey of robot manipulation in contact," *Robotics and Autonomous Systems*, vol. 156, p. 104224, 2022.
- [11] K. Kronander and A. Billard, "Stability considerations for variable impedance control," *IEEE Transactions on Robotics*, vol. 32, no. 5, pp. 1298–1305, 2016.
- [12] P. Y. Li and R. Horowitz, "Passive velocity field control of mechanical manipulators," *IEEE Transactions on robotics and automation*, vol. 15, no. 4, pp. 751–763, 2002.
- [13] —, "Passive velocity field control of (pvfc), part i. geometry and robustness," *IEEE Transactions on Automatic Control*, vol. 46, no. 9, pp. 1346–1359, 2001.
- [14] —, "Passive velocity field control of (pvfc), part ii. application to contour following," *IEEE Transactions on Automatic Control*, vol. 46, no. 9, pp. 1360–1371, 2001.
- [15] —, "Control of smart exercise machines. i. problem formulation and nonadaptive control," *IEEE IEEE/ASME Transactions On Mechatronics*, vol. 2, no. 4, pp. 237–247, 1997.
- [16] —, "Control of smart exercise machines. ii. self-optimizing control," *IEEE IEEE/ASME Transactions On Mechatronics*, vol. 2, no. 4, pp. 248–258, 1997.
- [17] F. Ferraguti *et al.*, "An energy tank-based interactive control architecture for autonomous and teleoperated robotic surgery," *IEEE Transactions on Robotics*, vol. 31, no. 5, pp. 1073–1088, 2015.
- [18] R. Rashad *et al.*, "Energy tank-based wrench/impedance control of a fully-actuated hexarotor: A geometric port-hamiltonian approach," in *2019 International Conference on Robotics and Automation (ICRA)*. IEEE, 2019, pp. 6418–6424.
- [19] Y. Michel *et al.*, "Passivity-based variable impedance control for redundant manipulators," *IFAC-PapersOnLine*, vol. 53, no. 2, pp. 9865–9872, 2020.
- [20] S. Haddadin and E. Shahriari, "Unified force-impedance control," *The International Journal of Robotics Research*, vol. 43, no. 13, pp. 2112–2141, 2024.
- [21] J. Seo *et al.*, "Geometric impedance control on SE(3) for robotic manipulators," *IFAC-PapersOnLine*, vol. 56, no. 2, pp. 276–283, 2023.
- [22] —, "A comparison between lie group-and lie algebra-based potential functions for geometric impedance control," *arXiv preprint arXiv:2401.13190*, 2024.
- [23] —, "Contact-rich SE(3)-equivariant robot manipulation task learning via geometric impedance control," *IEEE Robotics and Automation Letters*, 2023.
- [24] H. Ryu *et al.*, "Equivariant descriptor fields: SE(3)-equivariant energy-based models for end-to-end visual robotic manipulation learning," in *The Eleventh International Conference on Learning Representations (ICLR)*, 2023.
- [25] —, "Diffusion-EDFs: Bi-equivariant denoising generative modeling on SE(3) for visual robotic manipulation," *arXiv preprint arXiv:2309.02685*, 2023.
- [26] H. Huang *et al.*, "Fourier transporter: Bi-equivariant robotic manipulation in 3d," *arXiv preprint arXiv:2401.12046*, 2024.
- [27] J. Seo *et al.*, "SE(3)-equivariant robot learning and control: A tutorial survey," *arXiv preprint arXiv:2503.09829*, 2025.
- [28] R. M. Murray, Z. Li, and S. S. Sastry, *A mathematical introduction to robotic manipulation*. CRC press, 1994.
- [29] K. M. Lynch and F. C. Park, *Modern robotics*. Cambridge University Press, 2017.
- [30] F. Ferraguti *et al.*, "A tank-based approach to impedance control with variable stiffness," in *2013 IEEE international conference on robotics and automation*. IEEE, 2013, pp. 4948–4953.
- [31] K.-k. Lee and M. Buss, "Force tracking impedance control with variable target stiffness," *IFAC Proceedings Volumes*, vol. 41, no. 2, pp. 6751–6756, 2008.
- [32] F. Bullo and R. M. Murray, "Tracking for fully actuated mechanical systems: a geometric framework," *Automatica*, vol. 35, no. 1, pp. 17–34, 1999.
- [33] N. P. S. Prakash *et al.*, "Deep geometric potential functions for tracking on manifolds," in *2024 IEEE/RSJ International Conference on Intelligent Robots and Systems (IROS)*. IEEE, 2024, pp. i–viii.
- [34] —, "Variable impedance control using deep geometric potential fields," *IFAC-PapersOnLine*, vol. 58, no. 28, pp. 480–485, 2024.
- [35] T. Lee *et al.*, "Geometric tracking control of a quadrotor uav on se (3)," in *49th IEEE conference on decision and control (CDC)*. IEEE, 2010, pp. 5420–5425.
- [36] E. Todorov *et al.*, "Mujoco: A physics engine for model-based control," in *2012 IEEE/RSJ international conference on intelligent robots and systems*. IEEE, 2012, pp. 5026–5033.
- [37] M. Tadese *et al.*, "A two-step method for dynamic parameter identification of indy7 collaborative robot manipulator," *Sensors*, vol. 22, no. 24, p. 9708, 2022.